Original Article

MOLECULAR METABOLISM

Islet amyloid polypeptide does not suppress pancreatic cancer

Austin J. Taylor [1,2,3], **Evgeniy Panzhinskiy** [4,5], **Paul C. Orban** [1,2,6], **Francis C. Lynn** [1,6,7], **David F. Schaeffer** [3,8], **James D. Johnson** [4,7], **Janel L. Kopp** [4,7], **C. Bruce Verchere** [1,2,3,6,*]

ABSTRACT

Objectives: Pancreatic cancer risk is elevated approximately two-fold in type 1 and type 2 diabetes. Islet amyloid polypeptide (IAPP) is an abundant beta-cell peptide hormone that declines with diabetes progression. IAPP has been reported to act as a tumour-suppressor in p53-deficient cancers capable of regressing tumour volumes. Given the decline of IAPP during diabetes development, we investigated the actions of IAPP in pancreatic ductal adenocarcinoma (PDAC; the most common form of pancreatic cancer) to determine if IAPP loss in diabetes may increase the risk of pancreatic cancer.

Methods: PANC-1, MIA PaCa-2, and H1299 cells were treated with rodent IAPP, and the IAPP analogs pramlintide and davalintide, and assayed for changes in proliferation, death, and glycolysis. An IAPP-deficient mouse model of PDAC (*Iapp*$^{-/-}$; *Kras*$^{+/LSL\text{-}G12D}$; *Trp53*$^{flox/flox}$; *Ptf1a*$^{+/CreER}$) was generated for survival analysis.

Results: IAPP did not impact glycolysis in MIA PaCa-2 cells, and did not impact cell death, proliferation, or glycolysis in PANC-1 cells or in H1299 cells, which were previously reported as IAPP-sensitive. *Iapp* deletion in *Kras*$^{+/LSL\text{-}G12D}$; *Trp53*$^{flox/flox}$; *Ptf1a*$^{+/CreER}$ mice had no effect on survival time to lethal tumour burden.

Conclusions: In contrast to previous reports, we find that IAPP does not function as a tumour suppressor. This suggests that loss of IAPP signalling likely does not increase the risk of pancreatic cancer in individuals with diabetes.

Keywords Islet amyloid polypeptide; Amylin; Pancreatic ductal adenocarcinoma; Diabetes; Tumor suppressor

1. INTRODUCTION

Diabetes is associated with an increased relative risk in the majority of cancers [1,2]. Among the tissues with the highest increase in relative risk of cancer is the pancreas, with an approximately two-fold increase in both type 1 diabetes (T1D) [3] and type 2 diabetes (T2D) [1]. Pancreatic ductal adenocarcinoma (PDAC) is the most common form of pancreatic cancer [4], and approximately half of pancreatic cancer patients have diabetes at the time of diagnosis, with the majority of these having new-onset diabetes (diabetes diagnosis within 2 years preceding pancreatic cancer diagnosis) [5].

Although the association between diabetes and cancer has been recognized for decades, the mechanism connecting these two conditions has remained elusive. Obesity, hyperglycemia, inflammation, and hyperinsulinemia have all been reported as potential mechanisms through which diabetes may influence PDAC. Obesity and increased systemic inflammation, which are strongly associated with T2D, likely contribute to tumourigenesis [6] and elevated body mass index is associated with a modest increase in PDAC risk [7,8]. However, the relative risk for PDAC in T1D is comparable to that in T2D, suggesting that additional mechanisms beyond obesity contribute to the increased PDAC risk in diabetes. PDAC cells are highly glycolytic and hyperglycemia has been associated with PDAC, but this may be due to concurrent hyperinsulinemia and not elevated glucose per se [9]. The tumourigenic effects of insulin/IGF-1 signaling have been suggested to contribute to elevated PDAC in T2D (reviewed in [10,11]), and lowered insulin levels reduced pancreatic intraepithelial neoplasia (PanIN; a precursor lesion of PDAC) severity and area in a mouse model of PDAC initiation, in addition to altering pancreatic immune cell populations [12,13]. T1D is not characterized by hyperinsulinemia, however, suggesting that additional mechanisms may be driving the association between PDAC and diabetes.

Pancreatic blood flows from pancreatic islets to the acinar tissue, and then to the liver via the hepatic portal vein, resulting in over two-fold higher insulin concentrations in the hepatic portal vein than in arterial blood [14,15]. Thus, both acinar and hepatic tissues are exposed to locally increased levels of islet secretory products relative to systemic levels. Interestingly, the liver and pancreas are among the tissues with the highest cancer risk increase in T2D [1]. Given the tumourigenic actions of insulin and the reduction in PanINs that occur with reduced

[1]BC Children's Hospital Research Institute, Vancouver, BC, Canada [2]Centre for Molecular Medicine and Therapeutics, Vancouver, BC, Canada [3]Department of Pathology and Laboratory Medicine, University of British Columbia, BC, Canada [4]Life Sciences Institute, University of British Columbia, BC, Canada [5]Department of Biochemistry, University of British Columbia, BC, Canada [6]Department of Surgery, University of British Columbia, BC, Canada [7]Department of Cellular and Physiological Sciences, University of British Columbia, BC, Canada [8]Pancreas Centre BC, Vancouver, BC, Canada

*Corresponding author. BC Children's Hospital Research Institute, Vancouver, BC, Canada. E-mail: bverchere@bcchr.ca (C.B. Verchere).

Received June 10, 2022 • Revision received December 24, 2022 • Accepted January 2, 2023 • Available online 5 January 2023

https://doi.org/10.1016/j.molmet.2023.101667

insulin levels [12,13], it raises the possibility that islet secretory products altered in diabetes may influence PDAC initiation and growth and contribute to the increased relative risk of pancreatic cancer in diabetes. Islet amyloid polypeptide (IAPP) is an abundant beta-cell peptide and is stored and secreted from insulin-containing granules in a regulated pattern matching insulin secretion. Human IAPP is a highly aggregation-prone peptide with known toxicity. Similar to other amyloidogenic peptides, monomers and elongated fibrils show negligible toxicity, while intermediate oligomeric aggregates are thought to confer the majority of cellular toxicity [16–19]. Monomeric IAPP was, however, reported to have potent anti-tumour effects in p53-deficient cancers through inhibition of glycolysis and proliferation, and stimulation of apoptosis [20–22]. The non-aggregating FDA-approved IAPP analog, pramlintide, was reported to rapidly induce regression of p53-deficient thymic lymphomas in mice over a 3-week period with only twice-weekly injections [20]. In states of diabetes and beta-cell dysfunction, as found in T1D and advanced T2D, circulating IAPP levels are reduced [23–25]. If IAPP were to act as a tumour suppressor, reduced IAPP signalling may increase the risk of PDAC in diabetes.

The objective of this study was to determine whether IAPP acts as a tumour suppressor in PDAC, and whether IAPP deficiency as in diabetes may contribute to PDAC progression. We characterized the effects of monomeric IAPP peptides on proliferation, cell death, and glycolysis in the human pancreatic cancer cell lines PANC-1 and MIA PaCa-2, as well as the human non-small cell lung carcinoma cell line H1299 with previously shown sensitivity to IAPP. We also generated an IAPP-null mouse model of PDAC to determine whether physiological levels of IAPP influence PDAC growth *in vivo*.

2. MATERIALS AND METHODS

2.1. Animals

Congenic *Iapp*-null animals were generated by backcrossing $Iapp^{-/-}$ mice [26] in-house to C57BL/6J mice for >10 generations. The *Iapp* and *Kras* loci are both located on chromosome 6 in mice, separated by approximately 3 Mb. $Iapp^{-/-}$ mice were crossed to $Kras^{+/LSL\text{-}G12D}$ mice [27]. Heterozygous $Iapp^{+}Kras^{LSL\text{-}G12D}$ / $Iapp^{-}$ $Kras^{+}$ F1 mice were then crossed to $Iapp^{-}$ $Kras^{+}$ / $Iapp^{-}$ $Kras^{+}$ animals to screen for recombinant $Iapp^{-}$ $Kras^{LSL\text{-}G12D}$ / $Iapp^{-}$ $Kras^{+}$ offspring in the F2 generation. One recombinant F2 mouse was bred with $Trp53^{flox/flox}$; $Ptf1a^{+/CreER}$ mice [28,29] on a mixed CD1-C57BL/6J background. Experimental animals were generated through breeding the $Iapp^{-}$ $Kras^{LSL\text{-}G12D}$ / $Iapp^{+}Kras^{+}$; $Trp53^{flox/flox}$ animals with a separate colony of non-recombinant $Iapp^{+}Kras^{LSL\text{-}G12D}$ / $Iapp^{-}$ $Kras^{+}$; $Trp53^{flox/flox}$; $Ptf1a^{CreER/+}$ animals so that all experimental genotypes were generated from each breeding pair, enabling littermate controls.

The process of Kras expression and tumour development was initiated by three subcutaneous injections of tamoxifen (125 mg/kg; Toronto Research Chemicals; prepared in corn oil via sonication and filter sterilization) on alternating days beginning at P28-39. Humane endpoint was defined by 10% or greater body weight loss from maximum body weight, jaundice, and/or severely reduced activity levels. The presence of pancreatic tumours was confirmed by necropsy once the humane endpoint was reached. Both male and female mice were included in the study, and all experimental animals were housed in the Modified Barrier Facility at the University of British Columbia and fed PicoLab Rodent Diet 20 (5053) *ad libitum*. Blood glucose was measured using a OneTouch® UltraMini® (LifeScan, Inc.) glucometer and a small drop of blood collected from the distal tip of the mouse tail by lancing with a 25 G needle. Mice were cared for in accordance with the Canadian Council on Animals Care and studies were approved by the University of British Columbia Council on Animal Care.

2.2. Cell culture

PANC-1 cells were acquired from the laboratory of Dr. Wan Lam at the University of British Columbia, and maintained in ATCC-formulated DMEM (Gibco 11960 base medium supplemented with 10% FBS, GlutaMAX, sodium pyruvate, penicillin, and streptomycin). MIA PaCa-2 cells were acquired from ATCC and cultured in ATCC-formulated DMEM. H1299 cells were obtained from ATCC and cultured in ATCC-formulated RPMI-1640 (Gibco 11875 base medium supplemented with 10% FBS, glucose, HEPES, sodium pyruvate, penicillin, and streptomycin). Cells were cultured in a 37 °C, 5% CO_2, humidified incubator.

2.3. Peptides

Davalintide, pramlintide, and rIAPP peptides were obtained from MedImmune (Courtesy of Dr. James Trevaskis). Peptides were dissolved in 1,1,1,3,3,3-Hexafluoro-2-propanol (MilliporeSigma) at 1 mg/mL, lyophilized in single-use aliquots (50–200 μg/tube), and stored at −20 °C. Lyophilized peptide mass was confirmed by BCA assay (Thermo Scientific Pierce) of a sample tube from each lot after lyophilization. Lyophilized peptides were reconstituted in assay media for experiments.

2.4. Extracellular acidification rate

Extracellular acidification rate (ECAR) was assessed using a Seahorse XFe96 analyzer following manufacturer's protocols. PANC-1 cells were seeded in a Seahorse XF cell culture plate at a density of 1×10^4 cells / well in normal growth media and left overnight to adhere. Once adhered cells were treated for 48 h with 0.25–25 μM pramlintide, davalintide, or rodent IAPP (rIAPP) in complete growth media or media with reduced FBS (10%–0.1% FBS) and glucose (25 mM–2.5 mM glucose). After 48 h, cells were washed and incubated in Seahorse XF base medium (Agilent 102353-100) supplemented with GlutaMAX (2 mM final concentration) for 1 h in a non-CO_2 incubator at 37 °C. ECAR was measured in Seahorse XF base medium with 10 mM glucose (MilliporeSigma, G7021), 1 μM oligomycin (MilliporeSigma, O4876), and 50 mM 2-deoxy-glucose (MilliporeSigma, D8375). H1299 and MIA PaCa-2 cells were assayed similarly, except for seeding density (5×10^3 cells / well) and addition of 2 μM oligomycin was used during the assay. Glycolysis was measured by (maximum ECAR rate during glucose phase) − (last basal ECAR rate measured before glucose injection).

2.5. Cell death and proliferation

Cell death and proliferation were assayed using live cell imaging with nuclear live/dead stains. PANC-1 cells were seeded at a density of 4×10^3 cells / well on a 96-well ViewPlate® (PerkinElmer, 6005182) and adhered overnight. Once adhered, cells were washed in incubation media, and treated with 0.25–25 μM pramlintide, davalintide, or rIAPP in complete growth media lacking phenol red or media with reduced FBS (10%–0.1% FBS) and glucose (25 mM–2.5 mM glucose). Gemcitabine (MilliporeSigma, G6423) and cycloheximide (MilliporeSigma, C7698) were included as positive controls for cell death. Cells were labelled with Hoechst 33342 (0.05 μg/mL; Invitrogen) and propidium iodide (PI; 0.5 μg/mL; Invitrogen) for 1 h prior to commencing imaging. Cells were imaged every 2 h for up to 62 h (minimum 48 h) at 9 non-overlapping sites / well at 37 °C and 5% CO_2 on the Molecular Devices ImageXpress platform. Images were

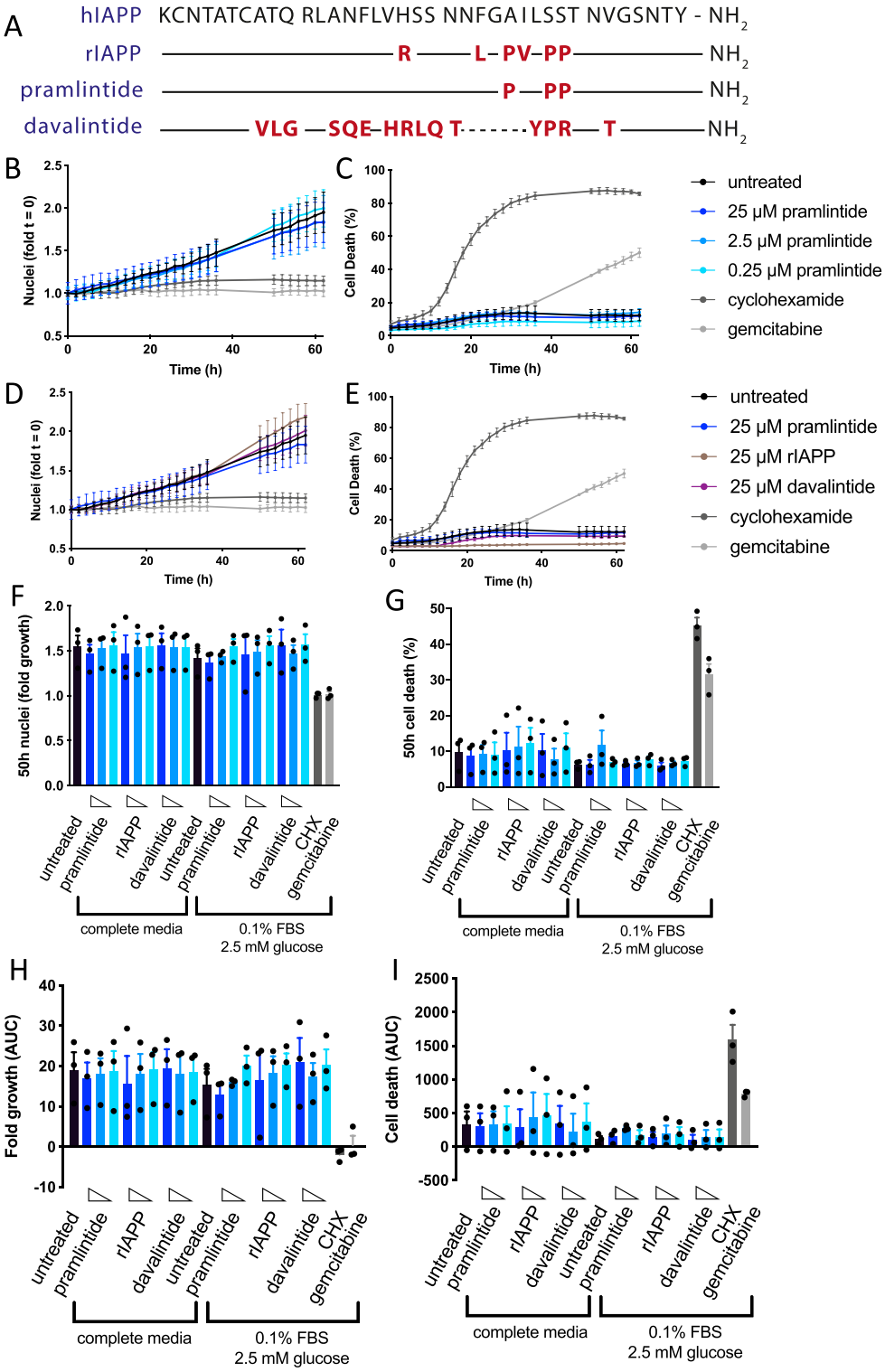

Figure 1: IAPP does not alter PANC-1 cell death or proliferation. (a) Alignment of human IAPP (hIAPP), rodent IAPP (rIAPP), pramlintide, and davalintide. All peptides are amidated at the C-terminus. (b,c) Representative plots showing proliferation and cell death responses in PANC-1 cells to a range of pramlintide concentrations in complete growth media for PANC-1 cells (error bars represent SD of technical triplicates from a single experiment). (d,e) Representative plots showing proliferation and cell death responses in PANC-1 cells to the highest pramlintide, rIAPP, or davalintide concentration (25 µM) in complete growth media for PANC-1 cells (error bars represent SD of technical triplicates from a single experiment). (f,g) Quantification of 3 independent proliferation and cell death experiments of PANC-1 cells after 50 h incubation with 25 µM (dark blue), 2.5 µM (blue), or 0.25 µM (light blue) rIAPP, pramlintide, or davalintide in either complete growth media or reduced glucose and FBS media (n = 3; error bars represent SD). (h,i) Alternate quantification of proliferation and cell death from (f,g) by area under the curve (AUC) from 0-50 h (n = 3; error bars represent SD). CHX, cycloheximide (1 mg/mL). Gemcitabine (5 µg/mL).

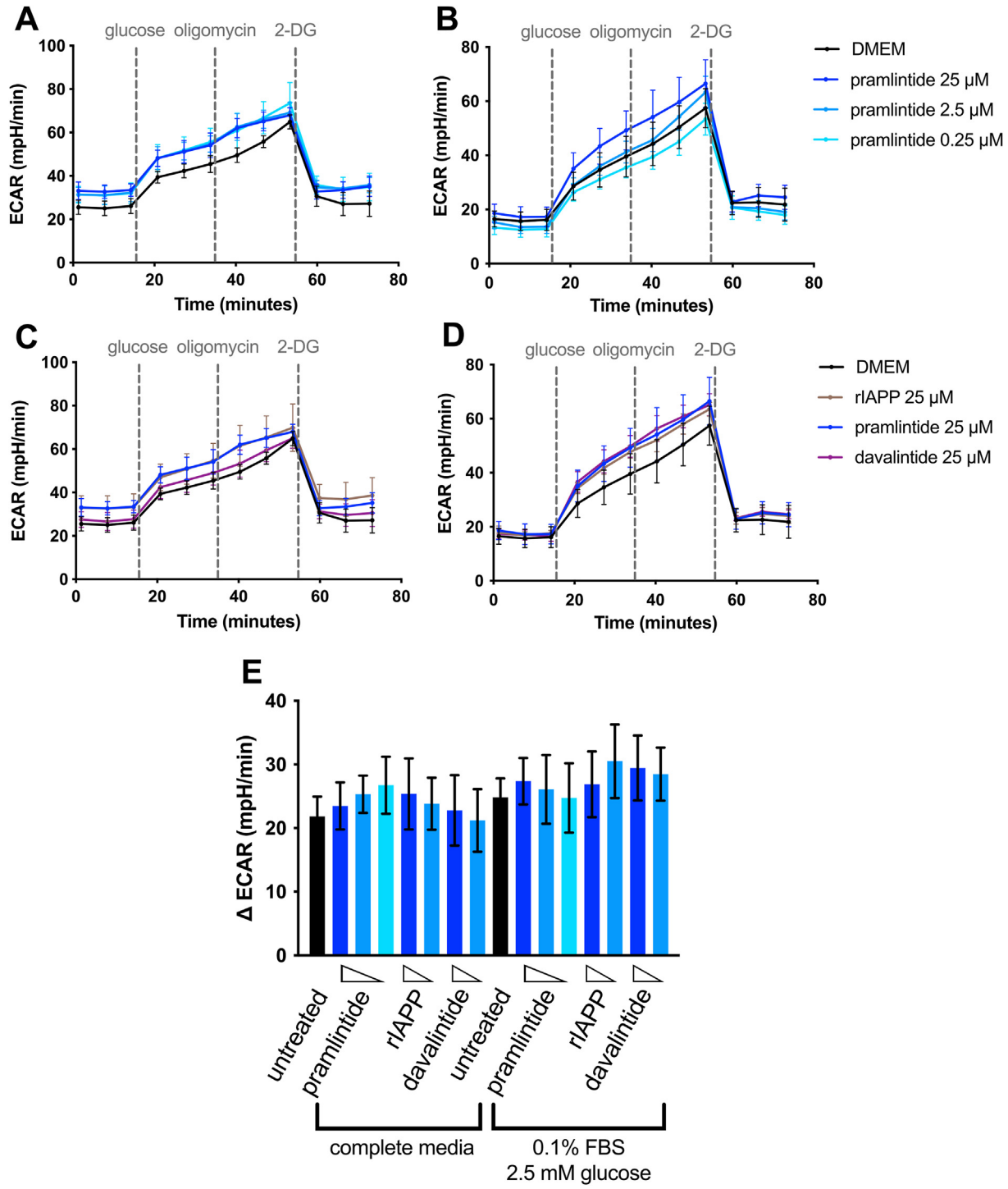

Figure 2: IAPP does not inhibit glycolysis in PANC-1 cells. (a,b) Representative extracellular acidification rate (ECAR) plots in PANC-1 cells cultured with pramlintide (0.25-25 μM) for 48 h in either complete growth media (a, 25 mM glucose and 10% FBS) or reduced FBS and glucose media (b, 2.5 mM glucose and 0.1% FBS) prior to analysis on a Seahorse XFe96 analyzer (error bars represent SD of 5-7 technical replicates from a single experiment). (c,d) Representative ECAR plots in PANC-1 cells cultured with pramlintide, rIAPP, or davalintide (25 μM) for 48 h in either complete or reduced glucose and FBS growth media as described in (a,b) (error bars represent SD of 5-7 technical replicates from a single experiment). (e) Quantification of glycolysis in n = 4 individual experiments with 25 μM (dark blue), 2.5 μM (blue), or 0.25 μM (light blue) pramlintide, rIAPP, or davalintide as indicated (error bars represent SD).

analyzed using MetaMorph analysis software. H1299 cells were assayed similarly, with a seeding density of 1×10^3 cells / well, and 0.2 μg/mL Hoechst 33342.

2.6. Pramlintide activity

HEK-293 cells stably transfected with a cAMP response element (CRE)-driven luciferase construct (pHTS-CRE) were kindly provided

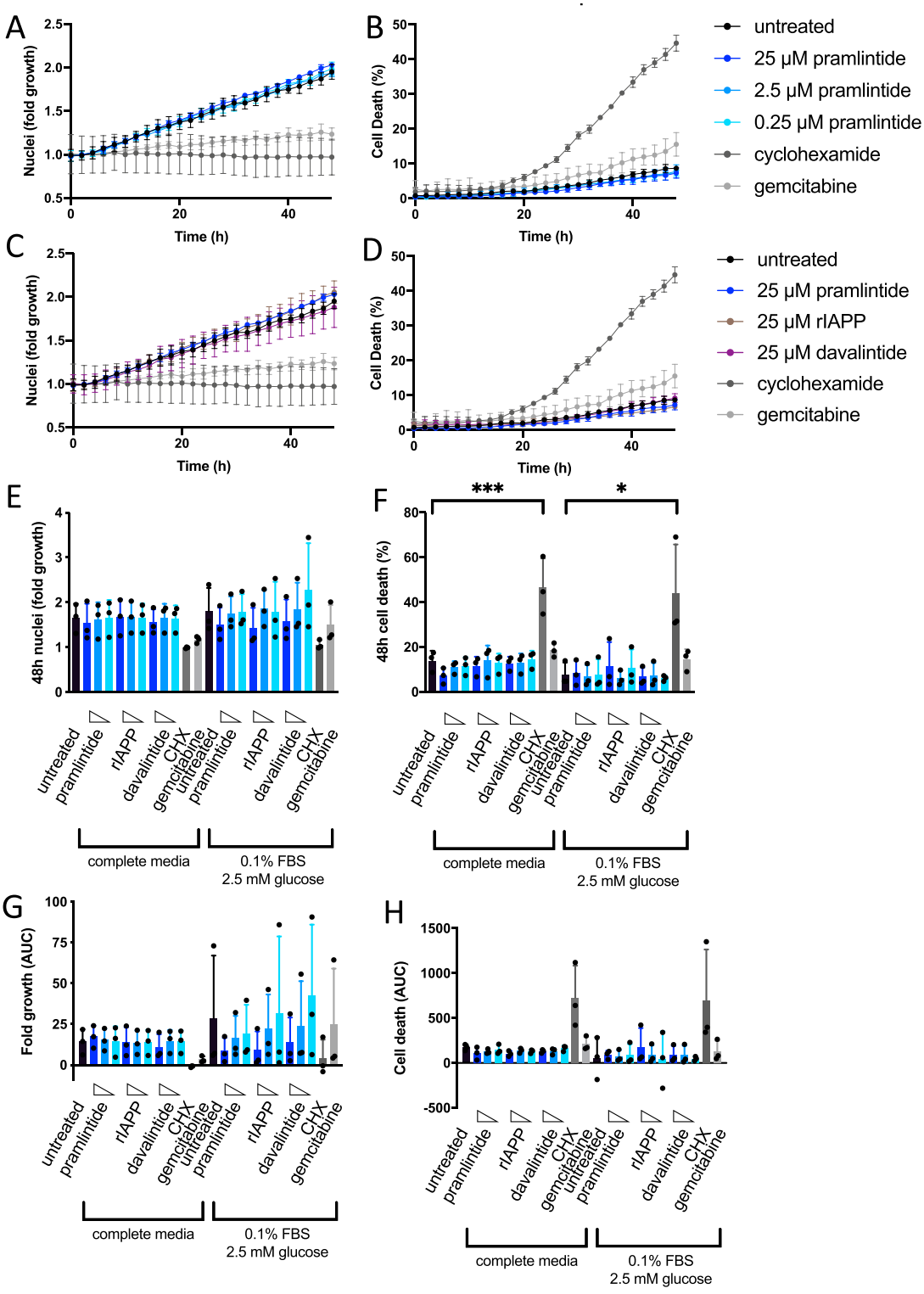

Figure 3: IAPP does not alter H1299 cell death or proliferation. (a,b) Representative plots showing proliferation and cell death of H1299 cells in response to a range of pramlintide concentrations in complete growth media for H1299 cells (error bars represent SD of technical triplicates from a single experiment). (c,d) Representative plots showing proliferation and cell death of H1299 cells in response to the highest pramlintide, rIAPP, or davalintide concentration (25 μM) in complete growth media for H1299 cells (error bars represent SD of technical triplicates from a single experiment). (e,f) Proliferation and cell death of H1299 cells in 3 independent experiments after 48 h incubation with 25 μM (dark blue), 2.5 μM (blue), or 0.25 μM (light blue) rIAPP, pramlintide, or davalintide in H1299 growth media as indicated (n = 3; error bars represent SD). (g,h) Alternate quantification of proliferation and cell death from (e,f) by area under the curve (AUC) from 0-48 h (n = 3; error bars represent SD). CHX, cycloheximide (0.5 mg/mL). Gemcitabine (5 μg/mL).

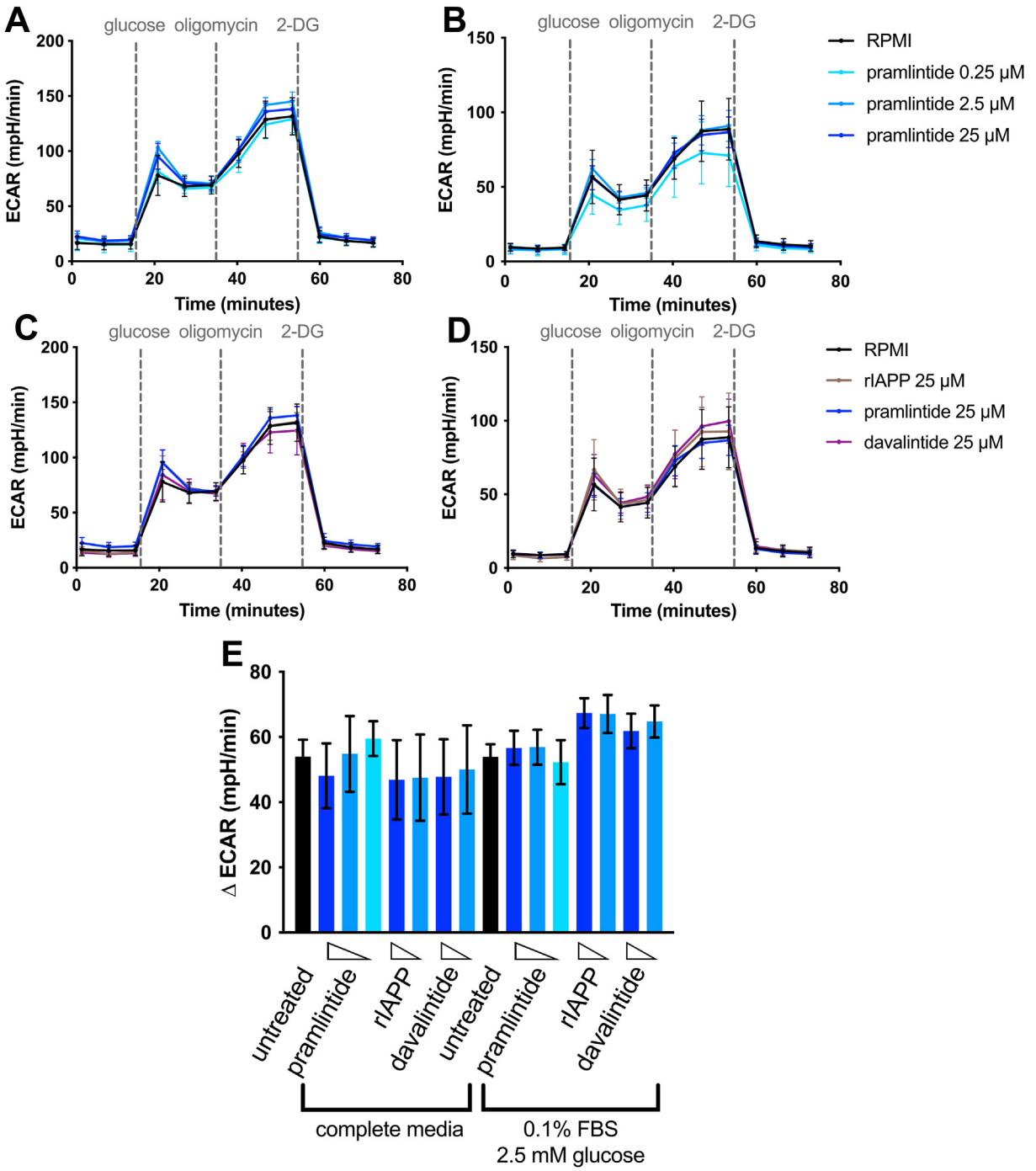

Figure 4: IAPP does not inhibit glycolysis in H1299 cells. (a,b) Representative extracellular acidification rate (ECAR) plots in H1299 cells cultured with pramlintide (0.25-25 μM) for 48 h in either complete growth media (a, 25 mM glucose and 10% FBS) or reduced FBS and glucose media (b, 2.5 mM glucose and 0.1% FBS) prior to analysis on a Seahorse XFe96 analyzer (error bars represent SD of 5-8 technical replicates from a single experiment). (c,d) Representative ECAR plots in H1299 cells cultured with pramlintide, rIAPP, or davalintide (25 μM) for 48 h in either complete or reduced glucose and FBS growth media as described in (a,b) (error bars represent SD of 5-8 technical replicates from a single experiment). (e) Quantification of glycolysis in n = 4 individual experiments with 25 μM (dark blue), 2.5 μM (blue), or 0.25 μM (light blue) pramlintide, rIAPP, or davalintide as indicated (error bars represent SD).

by the laboratory of Dr. Kieffer (University of British Columbia). A plasmid containing human *CALCR* and *RAMP3* sequences under a bidirectional promoter (pBI-hCALCR-hRAMP3) was generated in-house. A stable HEK-CRE-hCALCR-hRAMP3 cell line was developed by lipofectamine transfection of HEK-pHTS-CRE cells with linearized pBI-hCALCR-hRAMP3 followed by clonal expansion. HEK-CRE-hCALCR-hRAMP3 cells were seeded at 10^4 cells / well. Following overnight adherence, cells were washed with secretion assay buffer and incubated with pramlintide for 5 h. Following treatment, cells were lysed and luciferase expression analyzed using a Bright-Glo luciferase assay (Promega, E2610) following manufacturer protocol.

2.7. Pancreas histology and imaging

Mice were euthanized under surgical plane anesthesia by isoflurane inhalation. Pancreases and pancreatic tumours were dissected and fixed overnight at 4 °C in 4% paraformaldehyde and stored in 70% ethanol at 4 °C. Fixed pancreases were embedded in paraffin and sectioned 5 μm thick. Sections were rehydrated through series of xylene then ethanol washes, stained by hematoxylin and eosin, rehydrated through series of xylene then ethanol washes, and coverslips mounted with Permount (Fisher Chemical). Tiled brightfield images were acquired using a 10× objective on an Olympus B×61 microscope.

2.8. Statistical analysis

All data are presented as mean ± standard deviation and statistical analyses were performed using Prism8 or Prism9 statistical software (GraphPad). ANOVA followed by Fisher's least significant difference testing with Holm-Sidak multiple comparison corrections were used to compare experimental to control groups in Figures 1—4. Survival curves were compared by log-rank test. Statistical significance is displayed on figures as *$p < 0.05$, **$p < 0.01$, ***$p < 0.001$, ****$p < 0.0001$.

3. RESULTS

3.1. IAPP does not alter PANC-1 cell death or proliferation

Pramlintide, and davalintide [30] are monomeric IAPP analogs of rodent IAPP (rIAPP; Figure 1A) that do not aggregate but retain activity at human IAPP receptors [31]. To confirm that our peptide preparations were biologically active, we generated an IAPP-reporter cell line through stable transfection of an IAPP receptor (*CALCR* and *RAMP3*) into a HEK-293 cell line with cAMP response element (CRE)-regulated luciferase expression (Supplemental Fig. 1A). Pramlintide produced concentration-dependent IAPP receptor activation (luciferase expression) with an EC_{50} of 6.8 nM (Supplemental Fig. 1B), in agreement with reported values for the CALCR-RAMP3 receptor ranging from approximately 0.1—10 nM [31]. PANC-1 cells were treated with rIAPP, pramlintide, or davalintide at three concentrations in either standard complete growth media or low-glucose low-FBS media. As determined by time-lapse microscopy, pramlintide had no impact on proliferation or cell death at any of the three concentrations tested (Figure 1B&C), and neither rIAPP, pramlintide, nor davalintide inhibited proliferation or induced cell death even at the highest concentration (25 μM) tested (Figure 1D&E). No change in proliferation or cell death was observed when three individual experiments were analyzed at the 50-hour timepoint (Figure 1F&G) or by integration of the curves from 0 to 62 h (Figures 1H&I) with any concentration of the three tested IAPP monomers in either medium, while both positive controls (cycloheximide and gemcitabine) significantly induced cell death. Gemcitabine induced concentration-dependent cell death of PANC-1 cells, suggesting our cell death assay was sufficiently sensitive to detect both low and high levels of cell death (Supplemental Fig. 1C).

3.2. IAPP does not inhibit glycolysis in PANC-1 and MIA PaCa-2 cells

IAPP and pramlintide were previously reported to induce cell death and inhibit proliferation via inhibition of glycolysis [20]. To reassess this possibility, we cultured PANC-1 cells in complete media or low-FBS low-glucose media with multiple concentrations of pramlintide, rIAPP, or davalintide for 48 h, and analyzed glycolysis using a Seahorse XFe96 analyzer. Consistent with the lack of effects of these peptides on proliferation and cell death, neither pramlintide, rIAPP, nor davalintide inhibited PANC-1 glycolysis in either culture medium at any concentration (Figure 2A—D). Quantification of four individual experiments showed no effect of any IAPP peptide on PANC-1 glycolysis (Figure 2E). Pramlintide and rIAPP similarly had no effect on glycolysis in MIA PaCa-2 cells (Supplemental Fig. 2).

3.3. IAPP does not alter H1299 cell death or proliferation

Since the previous report of IAPP anti-tumour activity was in p53-null cell lines and PANC-1 and MIA PaCa-2 cells are p53 mutants, but not p53-null [32,33], we sought to confirm our observations in p53-null H1299 cells. We tested the effects of IAPP peptides on H1299 cells as with PANC-1 cells: three IAPP peptides at three concentrations each, in two different growth media, imaged approximately every 2 h for 48 h. As with PANC-1 cells, we observed no effect of 0.25—25 μM pramlintide (Figure 3A&B), nor of davalintide or rIAPP, on proliferation or cell death (Figure 3C&D). Quantification of proliferation and cell death at 48 h (Figure 3E&F) and by integration of the curves from 0 to 48 h (Figure 3G&H) revealed no effect of any of the IAPP peptides tested in either medium. Our confirmed biological activity of pramlintide (Supplemental Fig. 1A) and cell death assay sensitivity (Supplemental Fig. 1B) support our contention that monomeric IAPP does not impact proliferation or cell death in either H1299 or PANC-1 cells, and likely does not drive apoptosis in p53-null cells.

3.4. IAPP does not inhibit glycolysis in H1299 cells

Inhibition of glycolysis by IAPP was also previously reported by Venkatanarayan et al. in the p53-deficient H1299 cell line [20]. We assessed the impact of non-amyloidogenic IAPP peptides on glycolysis of H1299 cells. As in PANC-1 and MIA PaCa-2 cells, we observed no changes in glycolysis in H1299 cells pre-cultured for 48 h with pramlintide, rIAPP, or davalintide in standard complete media or low-FBS low-glucose media (Figure 4A—E). Our data suggest that IAPP that monomers do not inhibit glycolysis, regardless of p53 status.

3.5. IAPP deficiency does not impact survival in a mouse model of pancreatic ductal adenocarcinoma

To investigate the effects of physiological levels of IAPP *in vivo* on PDAC development, we generated an *Iapp*-null mouse expressing the conditional alleles $Kras^{LSL-G12D}$ and $Trp53^{flox}$, with tamoxifen-induced recombination directed to acinar tissue through $Ptf1a^{CreER}$. Tamoxifen was administered via three subcutaneous injections over 5 days beginning at 4—5 weeks of age to initiate PDAC development. Animals were monitored until humane endpoint. IAPP deficiency had no significant impact on survival, with median survival of 23.5 and 26 weeks post-tamoxifen in $Iapp^{+/+}$ and $Iapp^{-/-}$ animals, respectively (Figure 5A). The presence of tumours was confirmed at survival endpoint. $Kras^{+/LSL-G12D}$; $Trp53^{flox/flox}$; $Ptf1a^{+/CreER}$ mice displayed large fibrotic tumours regardless of *Iapp* expression, and *Iapp* deletion alone did not appreciably alter pancreas structure (Figure 5B). IAPP loss also did not result in sex-specific differences in survival (Supplemental Fig. 3A). As *Iapp* deletion has been reported to increase [26] or not alter body weight [34—37] in mice, we confirmed body weight and random-fed glycemia was unchanged in *Iapp*-null animals prior to the first humane endpoint (0—12 weeks post-tamoxifen; Supplemental Fig. 3B&C) to exclude any potential impact of increased adiposity or glycemia on tumour growth.

4. DISCUSSION

Our data do not support a role for monomeric IAPP signalling in suppression of pancreatic tumour growth. Neither pramlintide, rIAPP, nor

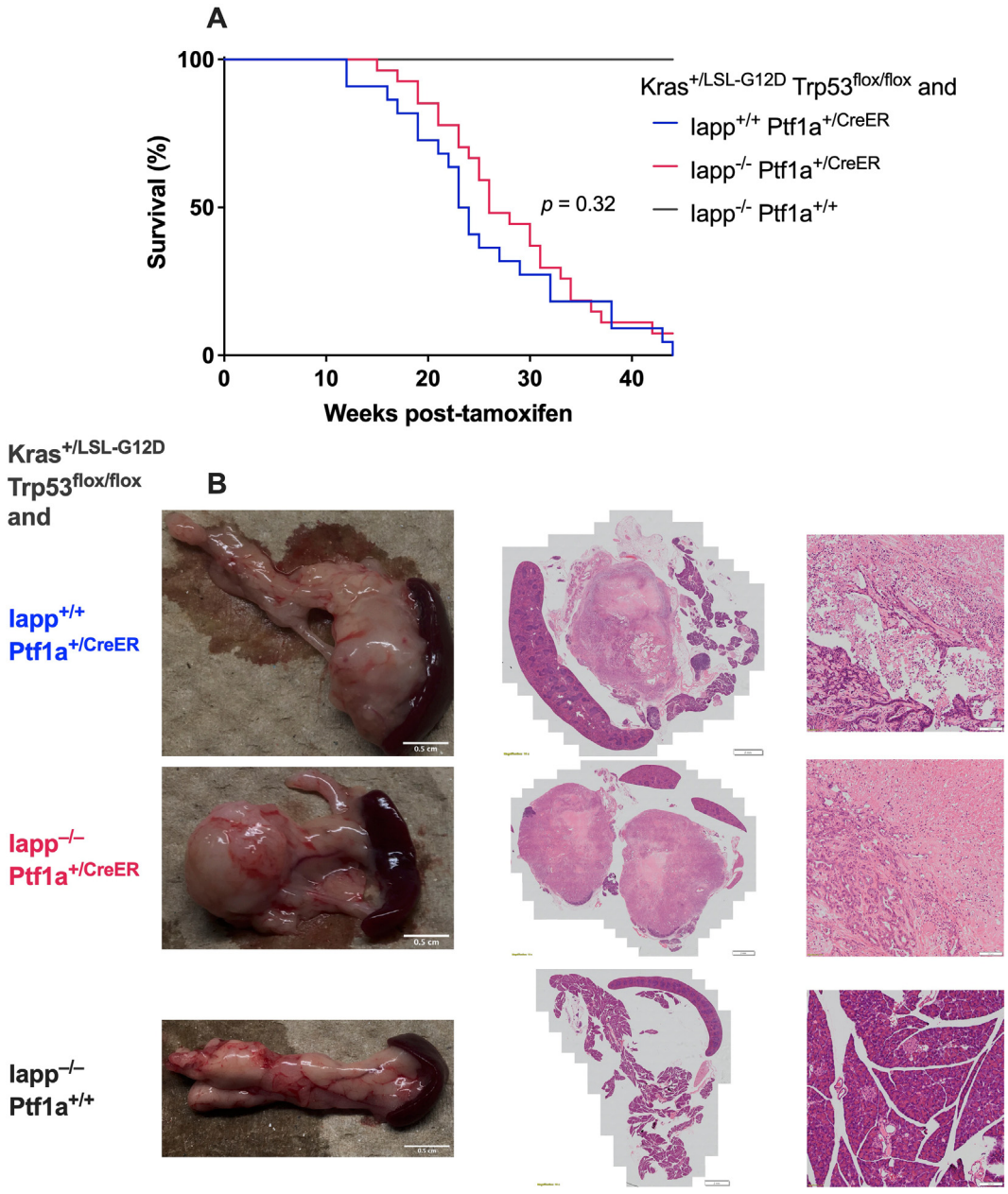

Figure 5: Physiological IAPP levels do not impact survival in a mouse model of pancreatic ductal adenocarcinoma (PDAC). (a) Tamoxifen was administered by 3 subcutaneous injections over 5 days beginning at P28-39. Animals were monitored weekly until humane endpoint was observed, and tumour presence was confirmed at necropsy in all *Ptf1a*$^{+/CreER}$ animals. Kaplan-Meier plot shows no significant difference between *Iapp-/-* (median survival 26 weeks) and *Iapp*$^{+/+}$ (median survival 23.5 weeks) animals in this mouse model of PDAC (*Kras*$^{+/LSL-G12D}$; *Trp53*$^{flox/flox}$; *Ptf1a*$^{+/CreER}$). n = 21-27, p = 0.32. (b) Both *Iapp*$^{-/-}$; *Kras*$^{+/LSL-G12D}$; *Trp53*$^{flox/flox}$; *Ptf1a*$^{+/CreER}$ and *Iapp*$^{+/+}$; *Kras*$^{+/LSL-G12D}$; *Trp53*$^{flox/flox}$; *Ptf1a*$^{+/CreER}$ mice develop pancreatic tumours with extensive fibrosis. Control *Iapp*$^{-/-}$; *Kras*$^{+/LSL-G12D}$; *Trp53*$^{flox/flox}$; *Ptf1a*$^{+/+}$ animals do not develop atypical pancreas morphology.

davalintide had any effect on PANC-1 proliferation, cell death, or glycolysis, and MIA PaCa-2 glycolysis was not impacted by rIAPP or pramlintide. Further, we were unable to reproduce previously reported findings that pramlintide inhibits glycolysis and proliferation, and induces cell death in H1299 cells [20]. We tested additional monomeric IAPP peptides with a range of concentrations spanning the concentration at which pramlintide was reported to have an effect in H1299 cells, and confirmed biological activity of our pramlintide preparations. For IAPP receptors, all six have reported EC_{50} values ranging from approximately 0.1—10 nM, depending on the specific IAPP receptor—ligand interaction [31]. All three IAPP peptides were tested at concentrations exceeding EC_{50} values, and we observed no effect of IAPP on cell death, proliferation, or glycolysis.

IAPP receptors are generated through heterodimerization of the calcitonin receptor (*CALCR*; CTR) with one of three receptor activity-modifying protein family members (RAMP-1,-2, or-3) which increase specificity of the receptors for IAPP [31]. Two major CTR splice variants exist in humans (CTR_a and CTR_b) [38], generating six possible IAPP

receptors when heterodimerized with one of 3 RAMP accessory proteins. CTR is a class B GPCR, with the dominant signalling pathway through G_s-coupled stimulation of adenylyl cyclase leading to cAMP production, although coupling also occurs with G_q proteins to drive activation of phospholipase C and mobilization of intracellular calcium stores [39,40]. RAMP association with CTR mainly alters ligand specificity rather than G-protein coupling and downstream signalling. However, RAMP-mediated modification of GPCR signalling is not entirely understood and CTR G-protein coupling and downstream signaling varies depending on the CTR variant and associated RAMP [40,41]. IAPP and IAPP receptor signalling is further complicated by IAPP activity (albeit relatively weak) on the calcitonin receptor-like receptor (*CALCRL*; CRLR) complexed with RAMP proteins [42,43], and signalling of several calcitonin family peptides (alpha- and beta-CGRP, adrenomedullin, intermedin, and calcitonin) through IAPP receptors [44].

Although studies on the actions of IAPP in cancer are limited, several studies have examined the effects of calcitonin, CGRP, and adrenomedullin, all of which can activate adenylyl cyclase through their respective receptors, and drive cAMP production in cells. Calcitonin has been shown not only to stimulate proliferation and metastasis of prostate cancer cells [45,46], but also to decrease ERK1/2 phosphorylation and tumour volume in cell-line based breast cancer transplant models in mice [47]. Adrenomedullin expression was found in pancreatic cancer cell lines, including PANC-1 cells, and adrenomedullin-overexpression in PANC-1 cells increased tumour growth in an orthotopic transplant model in mice despite undetectable levels of CRLR [48]. High adrenomedullin expression is also associated with poor outcome in PDAC, and adrenomedullin was found to enhance PDAC cell proliferation and invasion [48–50]. The divergent effects of these calcitonin-family peptides may be surprising at first, given their shared signalling pathways involving cAMP production and subsequent protein kinase A (PKA) activation. However when considering the vast number of PKA targets (>200) [51], it is plausible that cAMP-induced changes in proliferation and apoptosis are highly dependent on the expression and availability of PKA targets resulting from the specific tumour genomes and environments. The dual nature of cAMP as both a pro- and anti-apoptotic stimulus (reviewed in [52]) may be partly responsible for the discordance between the findings of this study and those of Venkatanarayan et al. [20] which reported tumour suppressor activity of IAPP.

Our *Iapp*-null mouse model of PDAC suggests no role of endogenous monomeric IAPP signaling in PDAC development and progression. However, at supraphysiological concentrations, IAPP analogs may impact the viability of cancerous cells indirectly through interactions with off-target receptors in stromal cells. Off-target activity or interaction with a thymic stromal population may explain the difference of our *in vivo* genetic deletion findings to those reported in the p53-deficient thymic lymphoma and pramlintide injection model [20]. IAPP activity on a thymic lymphoma stromal population may further require a p53-null stromal cell given the model used by Venkatanarayan et al. [20] was a global *Trp53*-null mouse. However, similar to human tumours, p53 loss in the $Iapp^{-/-}$; $Kras^{+/LSL\text{-}G12D}$; $Trp53^{flox/flox}$; $Ptf1a^{+/CreER}$ model is restricted to cancerous cells. Our data from *Iapp*-null PDAC mice suggest no direct impact of endogenous IAPP on tumour progression, and no impact of IAPP-derived therapeutics on human pancreatic cancer cell glycolysis, proliferation, or apoptosis.

5. CONCLUSIONS

In summary, our data indicate that it is unlikely that IAPP acts directly as a tumour suppressor in p53-null cancers, given the lack of impact IAPP and its tested analogs had *in vitro,* and similar PDAC incidences in IAPP null and wild-type mice. In view of the complex and diverging effects of cAMP signaling in tumours, it is reasonable to suppose that IAPP may directly influence cancer cell proliferation or apoptosis in cells expressing an IAPP receptor. However, we found no evidence for IAPP action in PANC-1 and MIA PaCa-2 cells, nor in the p53-null H1299 cells. The previously reported anti-tumour actions of monomeric IAPP may be highly restricted and dependent on tumour environment rather than broadly relevant to tumour biology or therapy.

Complete lack of IAPP, resulting from deletion of the *Iapp* gene, did not influence PDAC survival in our animal model. It thus seems unlikely that reduced IAPP signaling in T1D and T2D increases the risk, or worsens the prognosis, of PDAC. However, the benefits of exogenous IAPP analog therapy on body weight and glycemia management in diabetes may indirectly provide improved cancer outcomes in patients with diabetes. Further investigation of shared pathological features between T1D, T2D, and PDAC, such as pancreatic inflammation, may provide mechanistic insight and therapeutic approaches for diabetes and cancer.

AUTHOR CONTRIBUTIONS

All authors assisted with experiment design and interpretation. A.J.T. and E.P performed cell death experiments. A.J.T. and P.O. generated the HEK-CRE-hCALCR-hRAMP3 cells and performed the bioactivity assays. A.J.T. performed seahorse, mouse, histology, and microscopy experiments and analysis. C.B.V. devised and supervised project. A.J.T. and C.B.V. wrote the manuscript with editing contributions from all authors.

DATA AVAILABILITY

Data will be made available on request.

ACKNOWLEDGEMENTS

This work was supported by a Canadian Cancer Society Research Institute Innovation Grant and a Canucks for Kids Fund Diabetes Catalyst Grant. A.J.T was supported by a Canucks for Kids Fund graduate studentship and a Canada Graduate Scholarships Master's award. The authors would like to thank the following core facilities for facilitating experiments: BC Children's Hospital Research Institute cores for histology and microscopy, and University of British Columbia Modified Barrier animal facility. We also thank Debbie Hay (University of Otago) for expert advice on IAPP receptor biology and bioassays, the Kieffer Lab (University of British Columbia) for providing the HEK-CRE cells, and James Trevaskis (MedImmune) for providing pramlintide, rIAPP, and davalintide peptides.

CONFLICT OF INTEREST

The authors have no conflicts of interest to disclose.

APPENDIX A. SUPPLEMENTARY DATA

Supplementary data to this article can be found online at https://doi.org/10.1016/j.molmet.2023.101667.

REFERENCES

[1] Ling S, Brown K, Miksza JK, Howells L, Morrison A, Issa E, et al. Association of type 2 diabetes with cancer: a meta-analysis with bias analysis for unmeasured confounding in 151 cohorts comprising 32 million people. Diabetes Care 2020;43(9):2313–22. https://doi.org/10.2337/dc20-0204.

[2] Gordon-Dseagu VLZ, Shelton N, Mindell JS. Epidemiological evidence of a relationship between type-1 diabetes mellitus and cancer: a review of the existing literature. Int J Cancer 2013;132(3):501–8. https://doi.org/10.1002/ijc.27703.

[3] Stevens RJ, Roddam AW, Beral V. Pancreatic cancer in type 1 and young-onset diabetes: systematic review and meta-analysis. Br J Cancer 2007;96(3):507–9. https://doi.org/10.1038/sj.bjc.6603571.

[4] Klöppel G, Lüttges J. WHO-classification 2000: exocrine pancreatic tumors. Verhandlungen Der Deutschen Gesellschaft Fur Pathologie 2001;85:219–28.

[5] Pannala R, Leirness JB, Bamlet WR, Basu A, Petersen GM, Chari ST. Prevalence and clinical profile of pancreatic cancer–associated diabetes mellitus. Gastroenterology 2008;134(4):981–7. https://doi.org/10.1053/j.gastro.2008.01.039.

[6] Iyengar NM, Gucalp A, Dannenberg AJ, Hudis CA. Obesity and cancer mechanisms: tumor microenvironment and inflammation. J Clin Oncol 2016;34(35):4270–6. https://doi.org/10.1200/JCO.2016.67.4283.

[7] Larsson SC, Orsini N, Wolk A. Body mass index and pancreatic cancer risk: a meta-analysis of prospective studies. Int J Cancer 2007;120(9):1993e8. https://doi.org/10.1002/ijc.22535.

[8] Preziosi G, Oben JA, Fusai G. Obesity and pancreatic cancer. Surg Oncol 2014;23(2):61–71. https://doi.org/10.1016/j.suronc.2014.02.003.

[9] Wolpin BM, Bao Y, Qian ZR, Wu C, Kraft P, Ogino S, et al. Hyperglycemia, insulin resistance, impaired pancreatic β-cell function, and risk of pancreatic cancer. J Natl Cancer Inst 2013;105(14):1027–35. https://doi.org/10.1093/jnci/djt123.

[10] Zhang AMY, Wellberg EA, Kopp JL, Johnson JD. Hyperinsulinemia in obesity, inflammation, and cancer. Diabet Metab J 2021;45(3):285–311. https://doi.org/10.4093/dmj.2020.0250.

[11] Mutgan AC, Besikcioglu HE, Wang S, Friess H, Ceyhan GO, Demir IE. Insulin/IGF-driven cancer cell-stroma crosstalk as a novel therapeutic target in pancreatic cancer. Mol Cancer 2018;17:66. https://doi.org/10.1186/s12943-018-0806-0.

[12] Zhang AMY, Chu KH, Daly BF, Ruiter T, Dou Y, Yang JCC, et al. Effects of hyperinsulinemia on pancreatic cancer development and the immune microenvironment revealed through single-cell transcriptomics. Cancer Metabol 2022;10(1):5. https://doi.org/10.1186/s40170-022-00282-z.

[13] Zhang AMY, Magrill J, de Winter TJJ, Hu X, Skovsø S, Schaeffer DF, et al. Endogenous hyperinsulinemia contributes to pancreatic cancer development. Cell Metabol 2019;30(3):403–4. https://doi.org/10.1016/j.cmet.2019.07.003.

[14] Magkos F, Fabbrini E, Patterson BW, Eagon JC, Klein S. Portal vein and systemic adiponectin concentrations are closely linked with hepatic glucose and lipoprotein kinetics in extremely obese subjects. Metab Clin Exp 2011;60(11):1641–8. https://doi.org/10.1016/j.metabol.2011.03.019.

[15] Song SH, McIntyre SS, Shah H, Veldhuis JD, Hayes PC, Butler PC. Direct measurement of pulsatile insulin secretion from the portal vein in human Subjects1. J Clin ENdocrinol Metab 2000;85(12):4491–9. https://doi.org/10.1210/jcem.85.12.7043.

[16] Abedini A, Plesner A, Cao P, Ridgway Z, Zhang J, Tu L-H, et al. Time-resolved studies define the nature of toxic IAPP intermediates, providing insight for anti-amyloidosis therapeutics. Elife 2016;5:e12977. https://doi.org/10.7554/eLife.12977.

[17] Janson J, Ashley RH, Harrison D, McIntyre S, Butler PC. The mechanism of islet amyloid polypeptide toxicity is membrane disruption by intermediate-sized toxic amyloid particles. Diabetes 1999;48(3):491–8. https://doi.org/10.2337/diabetes.48.3.491.

[18] Zraika S, Hull RL, Verchere CB, Clark A, Potter KJ, Fraser PE, et al. Toxic oligomers and islet beta cell death: guilty by association or convicted by circumstantial evidence? Diabetologia 2010;53(6):1046–56. https://doi.org/10.1007/s00125-010-1671-6.

[19] Raleigh D, Zhang X, Hastoy B, Clark A. The β-cell assassin: IAPP cytotoxicity. J Mol Endocrinol 2017;59(3):R121–40. https://doi.org/10.1530/JME-17-0105.

[20] Venkatanarayan A, Raulji P, Norton W, Chakravarti D, Coarfa C, Su X, et al. IAPP-driven metabolic reprogramming induces regression of *p53*-deficient tumours *in vivo*. Nature 2015;517(7536):626–30. https://doi.org/10.1038/nature13910.

[21] Venkatanarayan A, Raulji P, Norton W, Flores ER. Novel therapeutic interventions for p53-altered tumors through manipulation of its family members, p63 and p73. Cell Cycle 2016;15(2):164–71. https://doi.org/10.1080/15384101.2015.1121333.

[22] Al-Keilani M, Alsmadi D, Darweesh R, Alzoubi K. Pramlintide, an antidiabetic, is antineoplastic in colorectal cancer and synergizes with conventional chemotherapy. J Clin Pharmacol 2018;10:23–9. https://doi.org/10.2147/CPAA.S153780.

[23] Courtade JA, Klimek-Abercrombie AM, Chen Y-C, Patel N, Lu PYT, Speake C, et al. Measurement of pro-islet amyloid polypeptide (1–48) in diabetes and islet transplants. J Clin ENdocrinol Metab 2017;102(7):2595–603. https://doi.org/10.1210/jc.2016-2773.

[24] Mäkimattila S, Fineman MS, Yki-Järvinen H. Deficiency of total and non-glycosylated amylin in plasma characterizes subjects with impaired glucose tolerance and type 2 diabetes. J Clin Endocrinol Metab 2000;85(8):2822–7. https://doi.org/10.1210/jcem.85.8.6721.

[25] Sanke T, Hanabusa T, Nakano Y, Oki C, Okai K, Nishimura S, et al. Plasma islet amyloid polypeptide (Amylin) levels and their responses to oral glucose in type 2 (non-insulin-dependent) diabetic patients. Diabetologia 1991;34(2):129–32. https://doi.org/10.1007/BF00500385.

[26] Gebre-Medhin S, Mulder H, Pekny M, Westermark G, Törnell J, Westermark P, et al. Increased insulin secretion and glucose tolerance in mice lacking islet amyloid polypeptide (amylin). Biochem Biophys Res Commun 1998;250(2):271–7. https://doi.org/10.1006/bbrc.1998.9308.

[27] Jackson EL, Willis N, Mercer K, Bronson RT, Crowley D, Montoya R, et al. Analysis of lung tumor initiation and progression using conditional expression of oncogenic K-ras. Genes Devlop 2001;15(24):3243–8. https://doi.org/10.1101/gad.943001.

[28] Marino S, Vooijs M, van Der Gulden H, Jonkers J, Berns A. Induction of medulloblastomas in p53-null mutant mice by somatic inactivation of Rb in the external granular layer cells of the cerebellum. Genes Devlop 2000;14(8):994–1004.

[29] Pan FC, Bankaitis ED, Boyer D, Xu X, Van de Casteele M, Magnuson MA, et al. Spatiotemporal patterns of multipotentiality in Ptf1a-expressing cells during pancreas organogenesis and injury-induced facultative restoration. Development 2013;140(4):751–64. https://doi.org/10.1242/dev.090159.

[30] Mack CM, Soares CJ, Wilson JK, Athanacio JR, Turek VF, Trevaskis JL, et al. Davalintide (AC2307), a novel amylin-mimetic peptide: enhanced pharmacological properties over native amylin to reduce food intake and body weight. Int J Obes 2010;34(2):385–95. https://doi.org/10.1038/ijo.2009.238.

[31] Bower RL, Hay DL. Amylin structure-function relationships and receptor pharmacology: implications for amylin mimetic drug development. Br J Pharmacol 2016;173(12):1883–98. https://doi.org/10.1111/bph.13496.

[32] Deer EL, González-Hernández J, Coursen JD, Shea JE, Ngatia J, Scaife CL, et al. Phenotype and genotype of pancreatic cancer cell lines. Pancreas 2010;39(4):425–35. https://doi.org/10.1097/MPA.0b013e3181c15963.

[33] Gradiz R, Silva HC, Carvalho L, Botelho MF, Mota-Pinto A. MIA PaCa-2 and PANC-1 – pancreas ductal adenocarcinoma cell lines with neuroendocrine differentiation and somatostatin receptors. Sci Rep 2016;6(1):21648. https://doi.org/10.1038/srep21648.

[34] Dacquin R, Davey RA, Laplace C, Levasseur R, Morris HA, Goldring SR, et al. Amylin inhibits bone resorption while the calcitonin receptor controls bone formation in vivo. J Cell Biol 2004;164(4):509–14. https://doi.org/10.1083/jcb.200312135.

[35] Turek VF, Trevaskis JL, Levin BE, Dunn-Meynell AA, Irani B, Gu G, et al. Mechanisms of amylin/leptin synergy in rodent models. Endocrinology 2010;151(1):143–52. https://doi.org/10.1210/en.2009-0546.

[36] Olsson M, Herrington MK, Reidelberger RD, Permert J, Gebre-Medhin S, Arnelo U. Food intake and meal pattern in IAPP knockout mice with and without infusion of exogenous IAPP. Scand J Gastroenterol 2012;47(2):191–6. https://doi.org/10.3109/00365521.2011.638392.

[37] Mollet A, Meier S, Grabler V, Gilg S, Scharrer E, Lutz TA. Endogenous amylin contributes to the anorectic effects of cholecystokinin and bombesin. Peptides 2003;24(1):91–8. https://doi.org/10.1016/S0196-9781(02)00280-2.

[38] Gorn AH, Lin HY, Yamin M, Auron PE, Flannery MR, Tapp DR, et al. Cloning, characterization, and expression of a human calcitonin receptor from an ovarian carcinoma cell line. J Clin Investig 1992;90(5):1726–35. https://doi.org/10.1172/JCI116046.

[39] Force T, Bonventre JV, Flannery MR, Gorn AH, Yamin M, Goldring SR. A cloned porcine renal calcitonin receptor couples to adenylyl cyclase and phospholipase C. Am J Physiol 1992;262(6 Pt 2):F1110–5. https://doi.org/10.1152/ajprenal.1992.262.6.F1110.

[40] Morfis M, Tilakaratne N, Furness SGB, Christopoulos G, Werry TD, Christopoulos A, et al. Receptor activity-modifying proteins differentially modulate the G protein-coupling efficiency of amylin receptors. Endocrinology 2008;149(11):5423–31. https://doi.org/10.1210/en.2007-1735.

[41] Moore EE, Kuestner RE, Stroop SD, Grant FJ, Matthewes SL, Brady CL, et al. Functionally different isoforms of the human calcitonin receptor result from alternative splicing of the gene transcript. Mol Endocrinol 1995;9(8):959–68. https://doi.org/10.1210/mend.9.8.7476993.

[42] Bühlmann N, Leuthäuser K, Muff R, Fischer JA, Born W. A receptor activity modifying protein (RAMP)2-dependent adrenomedullin receptor is a calcitonin gene-related peptide receptor when coexpressed with human RAMP1. Endocrinology 1999;140(6):2883–90. https://doi.org/10.1210/endo.140.6.6783.

[43] Poyner DR. International union of pharmacology. XXXII. The mammalian calcitonin gene-related peptides, adrenomedullin, amylin, and calcitonin receptors. Pharmacol Rev 2002;54(2):233–46. https://doi.org/10.1124/pr.54.2.233.

[44] Hay DL, Christopoulos G, Christopoulos A, Poyner DR, Sexton PM. Pharmacological discrimination of calcitonin receptor: receptor activity-modifying protein complexes. Mol Pharmacol 2005;67(5):1655–65. https://doi.org/10.1124/mol.104.008615.

[45] Shah GV, Rayford W, Noble MJ, Austenfeld M, Weigel J, Vamos S, et al. Calcitonin stimulates growth of human prostate cancer cells through receptor-mediated increase in cyclic adenosine 3',5'-monophosphates and cytoplasmic Ca2+ transients. Endocrinology 1994;134(2):596–602. https://doi.org/10.1210/endo.134.2.8299557.

[46] Shah GV, Thomas S, Muralidharan A, Liu Y, Hermonat PL, Williams J, et al. Calcitonin promotes in vivo metastasis of prostate cancer cells by altering cell signaling, adhesion, and inflammatory pathways. Endocr Relat Cancer 2008;15(4):953–64. https://doi.org/10.1677/ERC-08-0136.

[47] Nakamura M, Han B, Nishishita T, Bai Y, Kakudo K. Calcitonin targets extracellular signal-regulated kinase signaling pathway in human cancers. J Mol Endocrinol 2007;39(6):375–84. https://doi.org/10.1677/JME-07-0036.

[48] Ramachandran V, Arumugam T, Hwang RF, Greenson JK, Simeone DM, Logsdon CD. Adrenomedullin is expressed in pancreatic cancer and stimulates cell proliferation and invasion in an autocrine manner via the adrenomedullin receptor, ADMR. Cancer Res 2007;67(6):2666–75. https://doi.org/10.1158/0008-5472.CAN-06-3362.

[49] Keleg S, Kayed H, Jiang X, Penzel R, Giese T, Büchler MW, et al. Adrenomedullin is induced by hypoxia and enhances pancreatic cancer cell invasion. Int J Cancer 2007;121(1):21–32. https://doi.org/10.1002/ijc.22596.

[50] Hollander LL, Guo X, Salem RR, Cha CH. The novel tumor angiogenic factor, adrenomedullin-2, predicts survival in pancreatic adenocarcinoma. J Surg Res 2015;197(2):219–24. https://doi.org/10.1016/j.jss.2014.11.002.

[51] Isobe K, Jung HJ, Yang C-R, Claxton J, Sandoval P, Burg MB, et al. Systems-level identification of PKA-dependent signaling in epithelial cells. Proc Natl Acad Sci U S A 2017;114(42):E8875–84. https://doi.org/10.1073/pnas.1709123114.

[52] Insel PA, Zhang L, Murray F, Yokouchi H, Zambon AC. Cyclic AMP is both a pro-apoptotic and anti-apoptotic second messenger. Acta Physiol 2012;204(2):277–87. https://doi.org/10.1111/j.1748-1716.2011.02273.x.

